IEEE Access
Multidisciplinary | Rapid Review | Open Access Journal

Received February 16, 2019, accepted April 3, 2019, date of publication May 1, 2019, date of current version June 3, 2019.

Digital Object Identifier 10.1109/ACCESS.2019.2912511

Output Voltage Regulation of FC-UC Based Hybrid Electric Vehicle Using Integral Backstepping Control

MUHAMMAD SAUD KHAN, IFTIKHAR AHMAD, AND FARRUKH ZAIN UL ABIDEEN
National University of Sciences and Technology (NUST-SEECS), Islamabad, Pakistan
Corresponding author: Iftikhar Ahmad (iftikhar.rana@seecs.edu.pk)

ABSTRACT Depletion of hydrocarbons and increasing environmental pollution is pushing the researchers to work on finding some alternatives. Going for pure or hybrid electric vehicles (HEVs) seems a good option as it offers limitless energy option, which is environmentally friendly as well. In this paper, the contribution fuel cell is used as a primary/main source and an ultra-capacitor has been used as an auxiliary one, both connected to a dc bus through the dc–dc buck boost converter. This system harnesses energy from the sources as per the vehicle's demand. The supply of energy from both the sources has been controlled by the switches, for which integral backstepping-based nonlinear controller has been proposed. The Lyapunov theory-based analysis has been incorporated, which gives asymptotic stability of the entire system to track the reference signals. The comparison of the same HEV system of the proposed nonlinear technique has also been included in this paper using MATLAB/Simulink.

INDEX TERMS HEVs, fuel cell (FC), ultra-capacitor (UC), integral backstepping control technique.

I. INTRODUCTION

Use of fossil fuels in the conventional internal combustion engines (ICEs) resulted in environmental pollution and their depletion. These fuels are mainly used in vehicles which emit greenhouse gases (GHG); thus contributing to overall increasing the temperature of the universe. This situation is forcing the researchers working in control and automation of vehicles, to find some green and unending energy resources. Hybrid electric vehicles (HEVs) have got a lot of attraction due to zero GHG emission; thus are environmentally friendly [1]. Usually HEVs use a main and an auxiliary source; both responsible for catering the power demands of the vehicle. Fuel cell can be used as a main source as it gives electric energy without polluting the environment and gives economic solution as compared to ICEs [2].

The Ultra-Capacitor (UC) has been used as auxiliary source as it has the ability to charge and discharge very fast. The life time of FC is many times greater than conventional batteries and is a high power density source [3], [4]. These characteristics are needed when there are high and sudden load demands; for instance, the case when we need to accelerate the vehicle, during its starting or while there is steep ascent. It can be recharged when the energy produced by the FC is more than that required by the vehicle; for instance, during downhill motion or braking. Thus it is an excellent option to chose for continuously charging & discharging during varying load demands/transients. Actually it complements the main source for providing the power to the load without any problem.

Different combinations and topologies for the use of FCs, UCs and batteries in HEVs, have been proposed in the literature [5]. In [6], the author used multi-input sources connected to the DC bus and in [7], the author used bi-directional DC-DC converters connected to the DC bus whose voltage regulation is not catered. In [8]–[12], the each of the energy sources is connected to a DC-DC converter and has its own controller which make it a computationally and economically costly solution.

Multi-input HEVs have no such issue [13] and [14]; where all the energy input sources are controlled by a single controller. Though the proposed controller gives economic and computationally less costly solution but active power sharing between each source has not been considered.

Inherently, most DC-DC power converters are nonlinear in nature, specially when the parasitics resistances are

The associate editor coordinating the review of this manuscript and approving it for publication was Juntao Fei.

considered in the model. The derivations in [15], [16] clearly show that the averaged mathematical model of the DC-DC boost converter is nonlinear.

The authors in [17] and [18] used multi-input converter and designed a feedback proportional integral controller by linearizing the system around the reference point using small signal approximation. However, as discussed above, the DC-DC boost converter is itself nonlinear in nature. Therefore, using a linear approximation cannot give stable solution over a wide operating range of the converter [19] and hence the global stability of the system is doubtful. Thus the use of a nonlinear control scheme with a nonlinear mathematical model is the obvious choice [20]. There are, however, a few disadvantages, such as the nonlinear control scheme is computationally more complex and requires re-derivation each time there is a change in the mathematical model (such as an addition of another parasitic element in the model).

Using passive configuration of the DC bus, a Hysteresis based controller has been proposed for a battery-UC combination [21]. The resulting steady state response is oscillatory because of its bounds being controlled manually. In [22], an FC-UC topology has been proposed where the stability of the system has been linked to a energy management system, making it a bit computationally costly.

A passivity-based nonlinear controller with an estimator using Fuzzy logic rules to decide the amount of UC current required instantaneously has been proposed in [23]. It performs observing the state of charge of UC and fuel in FC. But Fuzzy logic controller depends on a set of rules. The Backstepping sliding mode control technique provides better results in terms of robustness [24].

The nonlinear backstepping control technique is a recursive one and a strict feedback form of the model is needed for its design. Backstepping Sliding Mode Control of FC-UC based Hybrid Electric Vehicle has recently been proposed in [20]. Integral control is a basic control for the feedback systems which has the ability to cater for parametric variations and slow time varying external disturbances [25]. The hybrid controller designed with the combination of integral control and conventional Backstepping control technique provides better robustness and removes steady state error. For air management of PEMFC systems using SMC, the reader is referred to [26].

In this research contribution, the integral of the tracking error ($e = x - x_d$) is added in the Lyapunov candidate function and the stability has been studied using Lyapunov based theory. The Integral Backstepping controller has been proposed in order to remove the steady state error which the conventional Backstepping controller has and performs far batter than the Lyapunov Redesign based nonlinear controller as well. The comparison of the proposed controller has been done with the other two using the MATLAB/Simulink which justify why we needed to propose it.

The remaining part of the paper has been arranged as follows: the section-II details about the topology and working of the proposed HEV. While the section-III details the construction of the HEV model and its parameters. Section-IV presents the analysis for the design of the Integral Backstepping controller and finally the controller itself. In section-V, the simulation results using MATLAB/Simulink have been presented to show the behavior of the proposed controller where it has been compared with some of the control technique given in the literature. Section-VI concludes the research contribution and presents the future work.

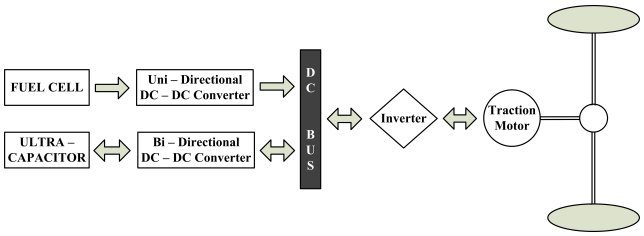

FIGURE 1. Schematic diagram for fuel cell hybrid electric vehicle under consideration.

II. DESCRIPTION OF THE FC-UC HEV

The HEV system considered for this research work is taken from [22] which consists of a Fuel Cell as a primary source and an Ultra-Capacitor as an auxiliary one as shown is Fig. 1. Here, the operation of the vehicle and the power flow with respect to both the source has been discussed.

A. FC CONVERTER

A fuel cell (FC) uses hydrogen fuel to produce electricity. It has no carbon emissions and produces water as a by-product, hence it is extremely environmentally friendly. The type of FC used in this study is Proton Exchange Membrane Fuel Cell (PEMFC or simply FC) because of its compact size and low startup time. FC is different from a chemical battery in many aspects, such as it cannot be recharged conventionally and it has a longer lifetime than battery. Therefore, a unidirectional DC-DC Boost converter is used with an FC. This Boost converter is used to step up the FC voltage to the required DC bus voltage (v_{dc}). It is also responsible for providing a steady and regulated v_{dc}. The FC boost converter has a single switch S_1, an inductor L_1 with its internal resistance R_1, and an output capacitor C_o (Fig. 2).

B. UC CONVERTER

An ultra-capacitor (UC) stores charge electrostatically and its electrical characteristics are very similar to a battery. However, it has some advantages over a battery: its charging and discharging rate (large power-density), bigger count of life-cycles of a UC [27], and large specific-power (though has small weight/size but can store large amount of energy). As we know that a UC can be recharged by power obtained from regenerative braking and downhill motion, a bi-directional DC-DC Boost-buck converter is connected with the UC. The name "*Boost-buck*" implies that this converter acts as a boost converter when the power flows from UC to the DC bus

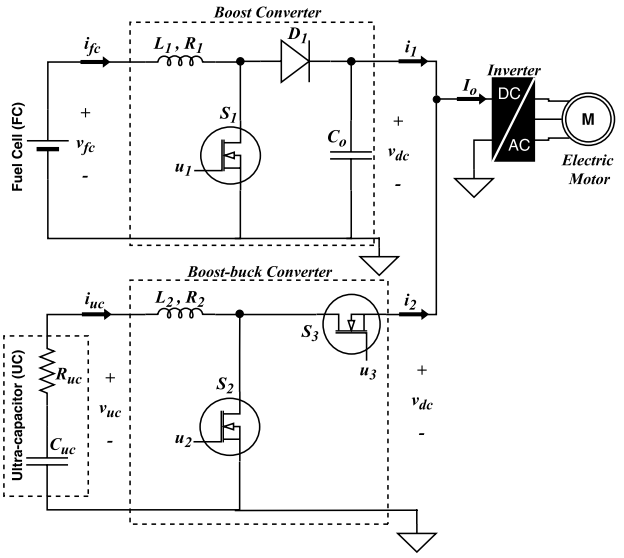

FIGURE 2. Circuit diagram of the DC power stage of the fuel cell HEV [22].

(UC discharging) and it acts as buck converter when the power flows from DC bus to the UC source (UC charging). It contains two switches S_2 & S_3 and one inductor L_2 with its internal resistance R_2, as depicted by the Fig. 2.

III. GLOBAL MATHEMATICAL MODEL

The global mathematical-model of the selected HEV system is derived and presented in [22], which is given as,

$$\begin{aligned}\dot{x}_1 &= -(1-U_1)\frac{x_3}{L_1} - \frac{R_1}{L_1}x_1 + \frac{V_{fc}}{L_1}\\ \dot{x}_2 &= -U_{23}\frac{x_3}{L_2} - \frac{R_2}{L_2}x_2 + \frac{V_{uc}}{L_2}\\ \dot{x}_3 &= (1-U_1)\frac{x_1}{C_o} + U_{23}\frac{x_2}{C_o} - \frac{I_o}{C_o}\end{aligned} \tag{1}$$

For the state-space model 1, the state variables/parameters and input parameters can be written as,

$$\begin{bmatrix}x_1 & x_2 & x_3\end{bmatrix}^T = \begin{bmatrix}< i_{fc} > & < i_{uc} > & < v_{dc} >\end{bmatrix}^T$$

&

$$\begin{bmatrix}U_1 & U_{23}\end{bmatrix}^T = \begin{bmatrix}< u_1 > & < u_{23} >\end{bmatrix}^T.$$

where, $< i_{fc} >$ = average FC current, $< i_{uc} >$ = average UC current, $< v_{dc} >$ = average value of DC-bus voltage, $< u_1 >$ = average control input parameter u_1, applied on the switch S_1, $< u_{23} >$ = average value of control input u_{23}. Here the state variables of the system are taken by averaging the corresponding quantities in which the passive elements stores energy, over one switching period [28]. u_1 & u_{23} are the control inputs which are the duty cycles of PWM applied to control the gates of MOSFET switches of the Buck-Boost converter. Their values lie in the interval [0, 1]. The model 1 is nonlinear MIMO system; making the control design complex.

The control u_{23} has been defined as

$$u_{23} = [(1-K)u_3 + K(1-u_2)], \tag{2}$$

where the control inputs u_2 and u_3 correspond to the switches S_2 and S_3 of the PWM respectively.

Also the buck and boost modes of the converter under consideration satisfy:

$$\begin{aligned}u_2 \in (0,1), \quad u_3 = 0\ (\text{off}) \qquad (\Longrightarrow \text{boost mode})\\ u_2 = 0\ (\text{off}), \quad u_3 \in (0,1) \qquad (\Longrightarrow \text{buck mode})\end{aligned}$$

Note that when UC empowers DC bus, then $i_{uc} > 0$ and when it is recharged regenerative braking or vehicle is going slower or during downhill motion, then $i_{uc} < 0$.

Now for I_{uc}^{ref} being the reference of UC current, we define a variable K representing the mode of UC as follows: $K = 1$ if $I_{uc}^{ref} > 0$ and $K = 0$ if $I_{uc}^{ref} < 0$

IV. DESIGN OF INTEGRAL BACKSTEPPING CONTROLLER

We are going to propose the Integral Backstepping controller for the DC bus voltage to be regulated without any steady state error under load transients and variations. We needed also to ensure that FC and UC continuously provide power to the load according to its demands. Finally the stability of the system should also be assured.

A. INDIRECT CURRENT CONTROL

The DC-DC boost converter exhibits a non-minimum phase response if the controller is used to track the v_{dc} voltage directly [22]. Hence to avoid this problem, an indirect current control using the current i_{fc} is proposed. The current i_{fc} is selected because the FC source remains operational throughout the whole vehicle operational time and it only provides uni-directional power. Therefore, it is much easier to provide the indirect current control using FC current i_{fc}. In order to achieve the indirect current control, the FC current reference, i_{fc}^{ref}, is generated in such a way that when i_{fc} is tracked to its reference i_{fc}^{ref} by the controller, the DC Bus voltage v_{dc} becomes equal to its reference v_{dc}^{ref}. The power equality equation is used to obtain the expression for the reference i_{fc}^{ref}.

$$\begin{aligned}P_{\text{in}} &= P_{\text{out}}\\ V_{fc}i_{fc} + V_{uc}i_{uc} &= v_{dc}I_o\\ \Rightarrow i_{fc}^{ref} &= \lambda\left[\frac{v_{dc}I_o - V_{uc}i_{uc}}{V_{fc}}\right]\end{aligned} \tag{3}$$

where, $\lambda > 1$ is the ideality factor that represents the losses in the power converters. Therefore, equation 3 shows the transformation of the voltage reference to the indirect current control reference.

First of all let's define the first tracking error as:

$$z_1 = x_1 - x_{1ref} \tag{4}$$

Taking time derivative of equation 4, we get:

$$\dot{z}_1 = -(1-u_1)\frac{x_3}{L_1} - \frac{r_1}{L_1}x_1 + \frac{V_{fc}}{L_1} - \dot{x}_{1ref} \tag{5}$$

Now, let's introduce the integral term given as:

$$\xi = \int_0^t (x_1 - x_{1ref})dt \tag{6}$$

Including the integral term in the first Lyapunov candidate function as:

$$V_{z_1} = \frac{1}{2}z_1^2 + \frac{\gamma}{2}\xi^2 \tag{7}$$

Taking time derivative of equation 7 and using equations 1 and 6, we have:

$$\begin{aligned}\dot{V}_{z_1} &= z_1\dot{z}_1 + \gamma\xi\dot{\xi} \\ &= z_1\left[-(1-u_1)\frac{x_3}{L_1} - \frac{r_1}{L_1}x_1 + \frac{V_{fc}}{L_1} - \dot{x}_{1ref} + \gamma\xi\right]\end{aligned} \tag{8}$$

To stabilize the system, we should have $\dot{V}_1 \leq 0$, so we take

$$-(1-u_1)\frac{x_3}{L_1} - \frac{r_1}{L_1}x_1 + \frac{V_{fc}}{L_1} - \dot{x}_{1ref} = -a_1 z_1$$

Here, a_1 is a positive constant. Selecting $\frac{x_3}{L_1}$ as the virtual control β and solving, we get:

$$\beta = \left(\frac{1}{1-u_1}\right)\left[a_1 z_1 - \frac{r_1}{L_1}x_1 + \frac{V_{fc}}{L_1} - \dot{x}_{1ref} + \gamma\xi\right] \tag{9}$$

Since β is only a virtual control and the combined system will only be stabilized when $\beta = \frac{x_3}{L_1}$, hence we define another error as:

$$z_2 = \frac{x_3}{L_1} - \beta \tag{10}$$

Using equation 10, the equation 5 becomes:

$$\begin{aligned}\dot{z}_1 &= -(1-u_1)(z_2+\beta) - \frac{r_1}{L_1}x_1 + \frac{V_{fc}}{L_1} - \dot{x}_{1ref} \\ &= -a_1 z_1 - (1-u_1)z_2 - \gamma\xi\end{aligned} \tag{11}$$

Therefore, equation 8 becomes:

$$\dot{V}_{z_1} = -a_1 z_1^2 - (1-u_1)z_1 z_2 \tag{12}$$

Now, taking time derivative of equation 10, we have:

$$\dot{z}_2 = \frac{\dot{x}_3}{L_1} - \dot{\beta} \tag{13}$$

For easier analysis, we first take the time derivative of β for which taking the time derivative of equation 9 and using the quotient rule, we get:

$$\begin{aligned}\dot{\beta} = \frac{\dot{u}_1}{(1-u_1)^2}&\left(a_1 z_1 - \frac{r_1}{L_1}x_1 + \frac{V_{fc}}{L_1} - \dot{x}_{1ref} + \gamma\xi\right) \\ &+ \frac{1}{(1-u_1)}\left(a_1\dot{z}_1 - \frac{r_1}{L_1}\dot{x}_1 - \ddot{x}_{1ref} + \gamma\dot{\xi}\right)\end{aligned}$$

By simplifying, we get

$$\dot{\beta} = \frac{\dot{u}_1\beta}{(1-u_1)} + \frac{1}{(1-u_1)}\Omega(z_1, z_2) \tag{14}$$

Here, $\Omega(z_1, z_2)$ is taken for the ease of calculation and is given as:

$$\begin{aligned}\Omega(z_1, z_2) = (a_1 - \frac{r_1}{L_1})[-a_1 z_1 - (1-u_1)z_2 - \gamma\xi] + \gamma z_1 \\ - \frac{r_1}{L_1}\dot{x}_{1ref} - \ddot{x}_{1ref}\end{aligned} \tag{15}$$

Hence using equations 1 and 14, the equation 13 can be written as:

$$\begin{aligned}\dot{z}_2 = \frac{1}{L_1}&\left[(1-u_1)\frac{x_1}{C_o} + u_{23}\frac{x_2}{C_o} - \frac{I_o}{C_o}\right] \\ &- \frac{\beta\dot{u}_1}{(1-u_1)} - \frac{\Omega(z_1, z_2)}{(1-u_1)}\end{aligned} \tag{16}$$

Using the composite Lyapunov function, we get:

$$V_{zc} = V_{z_1} + \frac{1}{2}z_2^2 \tag{17}$$

Taking the time derivative of equation 17, we get:

$$\begin{aligned}\dot{V}_{zc} &= \dot{V}_{z_1} + z_2\dot{z}_2 \\ &= -a_1 z_1^2 - z_2\left[(1-u_1)z_1 - \dot{z}_2\right]\end{aligned} \tag{18}$$

For $\dot{V}_{zc}$ to be negative definite, let:

$$(1-u_1)z_1 - \dot{z}_2 = a_2 z_2 \tag{19}$$

Here $a_2 > 0$ and the composite Lyapunov candidate function becomes:

$$\dot{V}_{zc} = -a_1 z_1^2 - a_2 z_2^2 \tag{20}$$

The equation 20 indicates that $\dot{V}_{zc} \leq 0 \quad \forall\, x \in \Re^n$. This ensures that the errors z_1 & z_2 decay exponentially with time and hence the desired tracking objective is achieved. To ensure $\dot{V}_{zc}$ remains negative definite, using equation 16, the equation 19 must be solved further to obtain:

$$\begin{aligned}\dot{u}_1 = \frac{1}{\beta}&[(1-u_1)a_2 z_2 - (1-u_1)^2 z_1 + (1-u_1)^2\frac{x_1}{L_1 C_o} \\ &+ (1-u_1)u_{23}\frac{x_2}{L_1 C_o} - (1-u_1)\frac{I_o}{L_1 C_o} - \Omega(z_1, z_2)]\end{aligned} \tag{21}$$

The term $\Omega(z_1, z_2)$ is taken for easier analysis and in given in equation 15.

So far, we have obtained a control law using Integral Backstepping control, which tracks the FC current (i_{fc} or x_1) and the DC bus voltage (v_{dc} or x_3) to their respective desired values. Now we will continue to obtain a control law to track the UC current (i_{uc}) to its reference value. Let's define another error as:

$$z_3 = x_2 - I_{sc}^{ref} \tag{22}$$

Taking the time derivative of equation 22 and using the equation 1, we have:

$$\begin{aligned}\dot{z}_3 &= \dot{x}_2 - \dot{I}_{sc}^{ref} \\ &= -u_{23}\frac{x_3}{L_2} - \frac{r_2}{L_2}x_2 + \frac{V_{sc}}{L_2} - \dot{I}_{sc}^{ref}\end{aligned} \tag{23}$$

Taking Lyapunov candidate function as:

$$V_{z_3} = \frac{1}{2}z_3^2 \tag{24}$$

Taking time derivative of equation 24 and using the equation 23, we get:

$$\dot{V}_{z_3} = z_3\left[-u_{23}\frac{x_3}{L_2} - \frac{r_2}{L_2}x_2 + \frac{V_{sc}}{L_2} - \dot{I}_{sc}^{ref}\right] \tag{25}$$

TABLE 1. Specifications and parametric values of main and auxiliary sources.

Source of power	Specs
PEMFC	Voltage-262 V Current-200 A Power-52 kW
UC-Module	2.5 V for single cell 82 cells in series 1500 F

TABLE 2. Component values of the DC-DC converters.

Parameter	Value
Inductors L_1&L_2	1 mH
Inductor resistance R_1&R_2	2 mΩ
Output Capacitance C_o	1 mF

Solving for u_{23}, we get the control law as:

$$u_{23} = \frac{1}{x_3}\left[L_2 a_3 z_3 - r_2 x_2 + V_{sc} - L_2 \dot{I}_{sc}^{ref}\right] \tag{26}$$

Here a_3 is a positive constant. Hence this is the final control law for the tracking of UC current obtained using integral Backstepping technique. The Lyapunov function in equation 24 can be included in the composite Lyapunov function V_{zc} present in equation 17, to obtain global asymptotic stability as shown in the equation below:

$$V_{zc_1} = -a_1 z_1^2 - a_2 z_2^2 - a_3 z_3^2 \tag{27}$$

For simulation purposes, the states x_1, x_2 and x_3 are supposed to be measurable without loss of generality. So, designing an observer for the estimation of state variables is not part of out research. These state variables are voltages of the capacitors and the currents of the inductors which are measurable with the help of voltmeter and ammeter.

V. SIMULATION RESULTS

Here we have presented few simulation results for the proposed control scheme of a hybrid electric vehicle using MATLAB/Simulink software.

A. CHOICE OF PARAMETERS FOR THE SIMULATIONS

For the purpose of comparison of the proposed controller with those given in the literature, we have taken the same specifications and parametric values as given in [22] which are presented in the form of a table (1).

The parametric values of the DC-DC converters have been detailed in Table 2. In order to justify the validity of proposed controller in the simulation results, we have consider the same data as considered by [20] and [22].

The parametric values for the simulations (3) have been chosen on the basis of hit & trial, since they can't be evaluated by some systematic manner. Being gains, they are supposed to be having positive values.

TABLE 3. Parametric values and gains.

Controller type	Parameter	Value
Backstepping Controller	k_1	1000
	k_2	100
	k_3	1000
Integral Backstepping Controller	a_1	1000
	a_2	1000
	a_3	1000
	γ	100

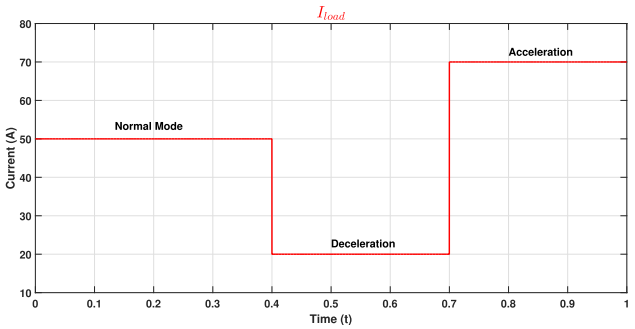

FIGURE 3. Applied motor load current of the vehicle I_o.

B. OUTPUT GRAPHS AND ANALYSIS OF RESULTS

The results of this HEV system are presented in the Figs. 3–20. The simulation results are divided into three parts: The first part illustrates the system's behavior using conventional Backstepping control scheme. The second part shows system's response when using Integral Backstepping controller. The third part provides a comparison between a previous study [22] and the proposed scheme.

1) SIMULATION RESULTS FOR BACKSTEPPING CONTROLLER

Figure 3 shows the varying load transients for different vehicular cycles. High current shows acceleration, normal current represents normal vehicular operation, whereas low load describes deceleration and regenerative braking duration.

The figures 4, 5 & 6 show asymptotic convergence of the states to their references signals. This represents that our desired objective is achieved. It is observed from the figures that initially the maximum value of current of the fuel cell goes to 300 A as shown in the fig. 5. Few transients have been observed for a short time interval (0.04 sec) which may be taken as settling time of the proposed controller. Later on, the variations in states occur at time instants when the load current I_o changes its value. However, after a very short interval of time, the states eventually converge to their references.

For simplicity, the UC current has been kept constant. The reference value for UC current I_{UC}^{ref} has been given 10 A, which it tracks very nicely. Moreover, the initial start-up power is supplied by the UC which can be seen in the fig. 6.

Figs. 7 & 8 show the DC Bus voltage v_{dc}, tracking its reference value of 400V DC. Slight variations can be observed at time instants where the I_o changes its value.

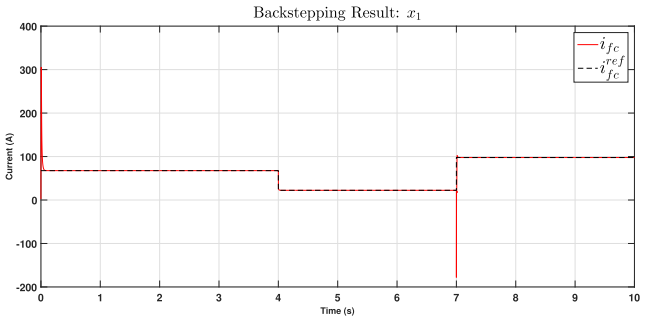

FIGURE 4. Plot of backstepping state $x_1 = i_{fc}$.

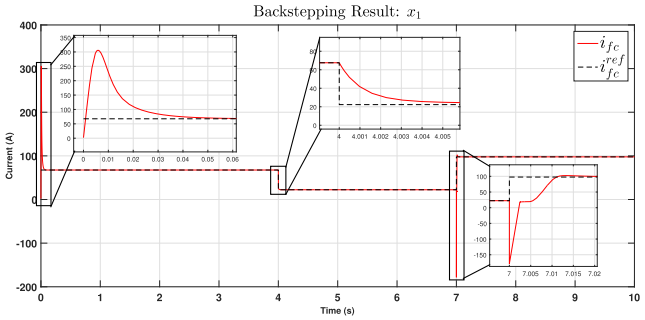

FIGURE 5. Zoomed-in view of backstepping state $x_1 = i_{fc}$.

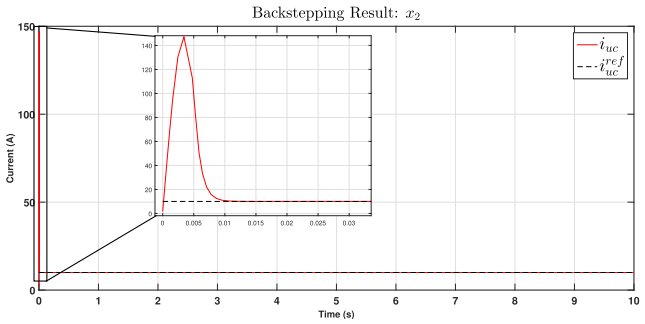

FIGURE 6. Zoomed-in view of backstepping state $x_2 = i_{uc}$.

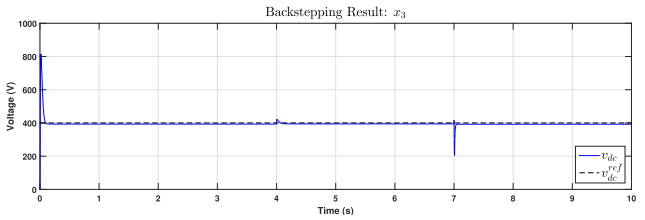

FIGURE 7. DC bus voltage under varying load conditions (backstepping controller).

Figure 9 shows the control signals applied at the gate of MOSFET switches.

2) SIMULATION RESULTS FOR INTEGRAL BACKSTEPPING CONTROLLER

In this simulation part, first of all the integral Backstepping controller has been used to carry out the similar vehicular operations with the same load demands as given in V-B1. The control scheme is kept same with all the current and voltage references same as given in the simulation part V-B1.

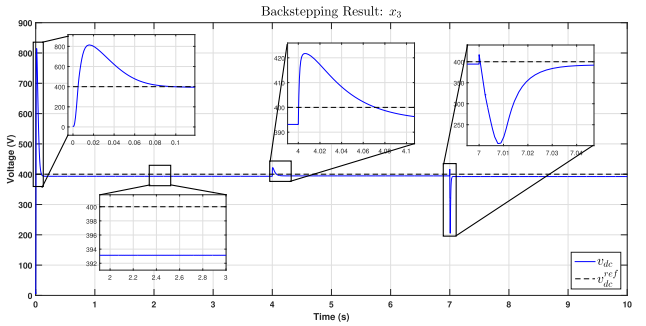

FIGURE 8. Zoomed-in view of state $x_3 = v_{dc}$ (backstepping controller).

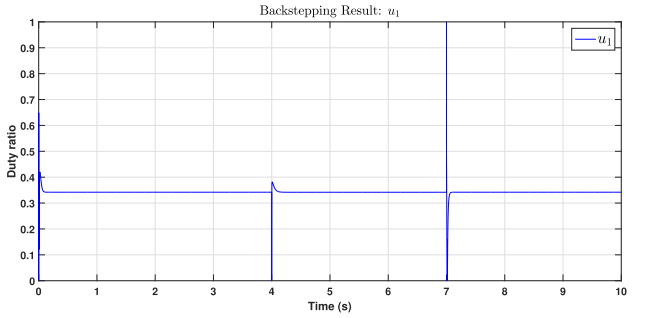

(a)

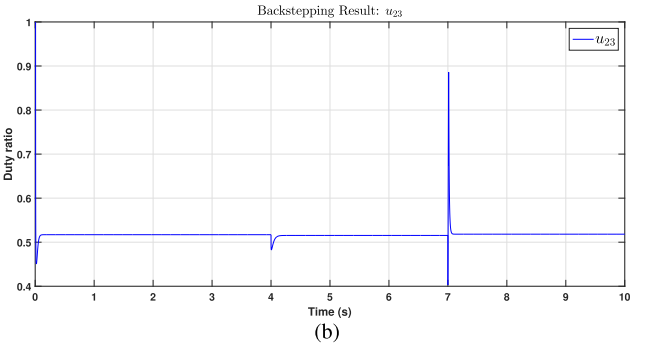

(b)

FIGURE 9. Control signals for the backstepping controller. (a) Plot of duty ratio u_1. (b) Plot of duty ratio u_{23}.

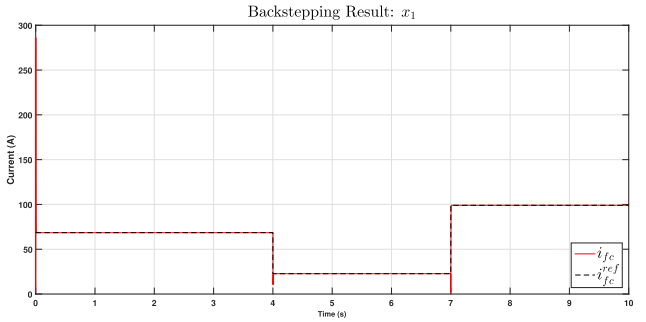

FIGURE 10. Plot of integral backstepping state $x_1 = i_{fc}$.

This is used to compare the performance of the Backstepping controller and the proposed integral Backstepping controller. The proof of efficient reference tracking of the state variables can be seen in the figures 10 and 11. Hence, the stability of the system and its performance are satisfactory in this simulations.

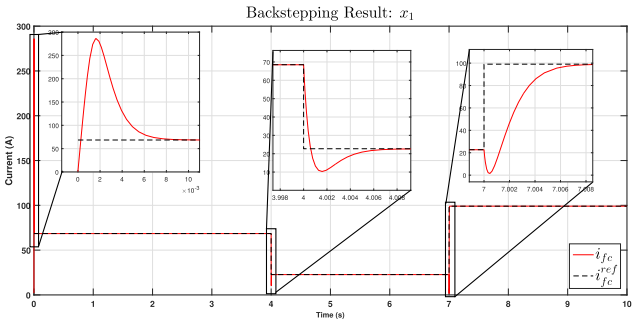

FIGURE 11. Zoomed-in view of integral backstepping state $x_1 = i_{fc}$.

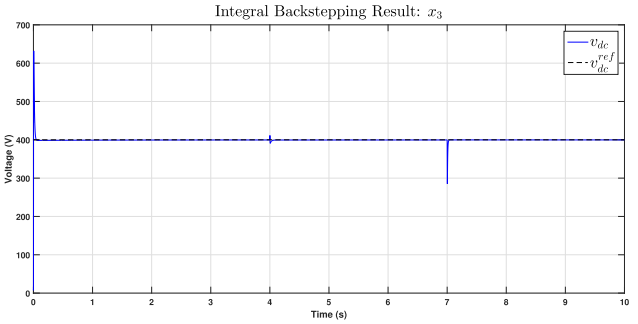

FIGURE 12. DC Bus voltage under varying load conditions (integral backstepping).

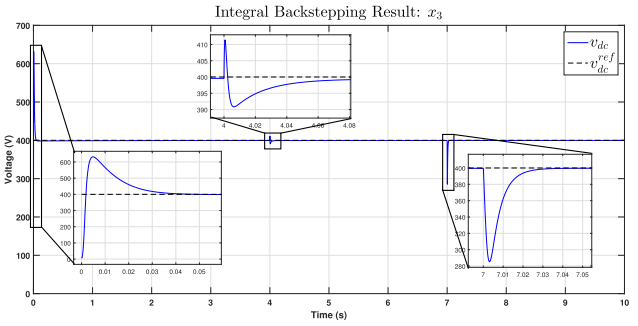

FIGURE 13. Zoomed-in view of state $x_3 = v_{dc}$ (integral backstepping controller).

The plots of state variables i_{uc} & i_{fc} can be seen in figure 10. It is worth noticing that the ultra capacitor's current i_{uc} has been kept at a constant value of 10 A for this part of the simulations and the FC current provides the remaining load current. Slight variations can be observed in the fig. 11 at the time interval where the load changes. However, the proposed controller make it stable in very small span of time.

The plot of DC Bus voltage v_{dc} is shown in figs. 12 & 13. Here, the DC Bus voltage is steady, regulated and achieves its reference value of 400 V very nicely. When compared with the v_{dc} waveform for Backstepping controller (fig. 13), integral backstepping controller provides an output DC bus voltage with less steady state error and lower values of initial transients as can be seen in the fig. 13. Expectedly, the transients of the state x_3 (or v_{dc}) correspond to the transients of the state x_1 (or i_{fc}) because of the indirect current control approach, as illustrated in figs. 13 & 11 respectively.

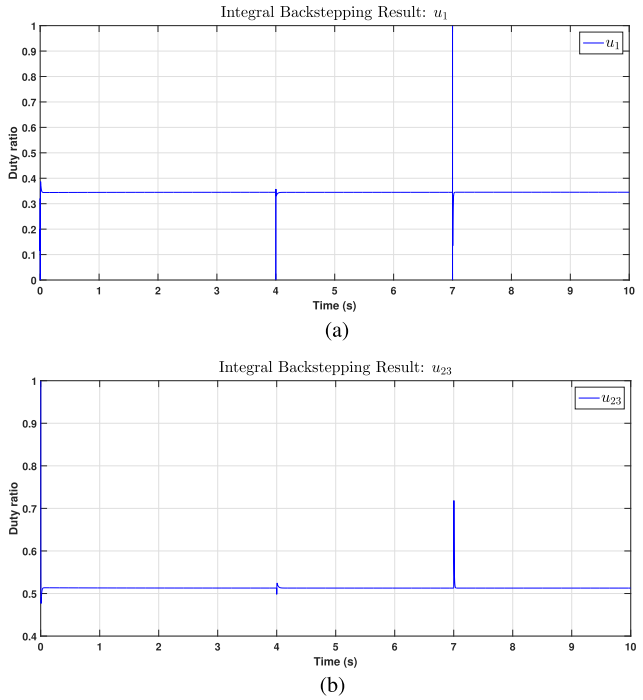

FIGURE 14. Plots of control signals (integral backstepping controller). (a) Plot of duty ratio u_1. (b) Plot of duty ratio u_{23}.

Figure 14a shows that the dip in the graph at 0.7 sec. The dip in the graph is due to load current changes i.e. deceleration mode to acceleration mode. At 10 sec, the vehicle is at acceleration mode so the duty cycle u_{23} remains constant. Figure 14 shows the plots of control inputs u_1 & u_{23} which have been used in the MOSFET.

So far we have kept i_{uc} constant and provided the load transients using i_{fc}. Now for the baseline power from fuel cell, a constant current has been provided to the system. The load transients are provided by the UC source.

Now in order to justify the contribution, the performance of the proposed control scheme has been tested for EUDC (European Extra-Urban Driving Cycle). It is thought to be a standard method to validate the results for the hybrid electric vehicles. The speed profile of the EUDC has been presented in Fig. 15. The acceleration or high speed mode represents the high motor load and deceleration or low speed mode represents low motor load.

The profile of the load current I_o for EUDC has been shown in Fig. 18. This profile has been produced considering the supposed specification of the vehicle, the characteristics of the inverter having 75 per cent efficiency and that of induction motor. The following equation relates the specifications of the vehicle with the load current.

$$I_o = \frac{1}{V_{ref} \times \eta_{inverter}} \left[\frac{1}{2} \rho_{air} v_t^2 A C_x + M_t g C_r + M_t \frac{dv_t}{dt} \right] v_t \tag{28}$$

where, V_{ref} is reference DC Bus voltage to be tracked, v_t is vehicle's speed and ρ_{air} represents the density of air. Other parameters have been tabulated in 4.

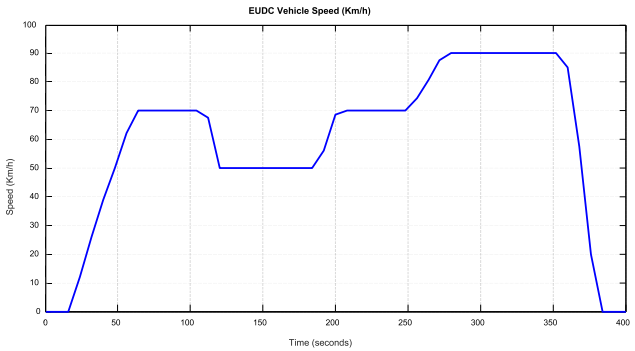

FIGURE 15. Profile of vehicle's speed in EUDC.

TABLE 4. Specifications of the inverter, motor, & vehicle.

Parameter	Value
Total mass of the vehicle M_t	1922 kg
Aerodynamic drag coefficient C_x	0.3
Vehicle frontal area A	2.5 m^2
Rolling resistance coefficient C_r	0.01
Gravitational acceleration constant g	9.8 m/s^2
Inverter efficiency $\eta_{inverter}$	75%

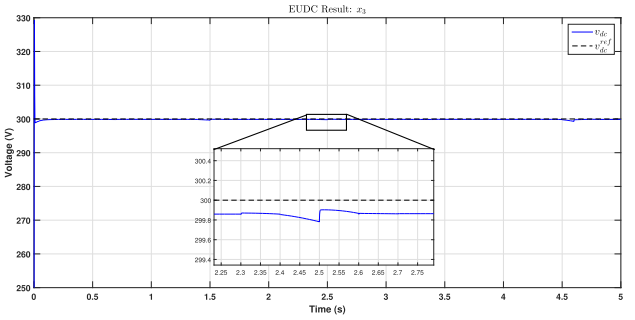

FIGURE 16. DC-bus voltage when the load conditions of EUDC is varying.

Now to make it computationally less costly, we have supposed 400 seconds equivalent to 5 seconds without disturbing the curve of the profile of the load. This supposition is justified by the fact that it UC which is responsible for meeting the load transients and not the FC which provide a constant current.

The tracking of DC-Bus voltage v_{dc} to its reference value of 300V DC has been shown in Fig. 16. This figure show that there are few but negligibly small oscillations at the time intervals where the load current I_o has been varied. The zoomed part shows that the steady state error in case of integral Backstepping controller is negligibly small which shows the importance of this control scheme when compared with the conventional Backstepping control scheme. It proves efficient DC bus voltage regulation using proposed scheme.

The plots of state variables i_{uc} & i_{fc} can be seen in figs. 17 and 18 respectively. It is being noticed that the FC current i_{fc} is providing the nominal power, which is used to drive the vehicle load in normal cruising mode and again the UC current charges the additional required load current. A simple power split can also be observed in figs. 17 and 18.

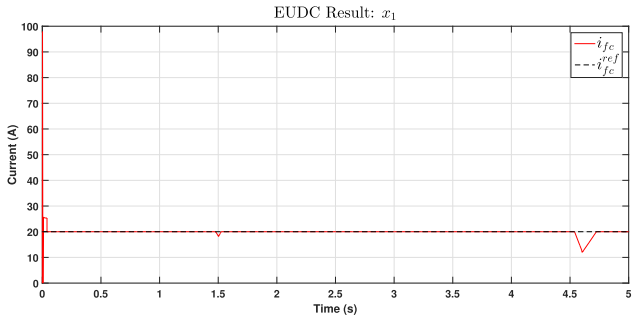

FIGURE 17. Plot of state i_{fc} (EUDC).

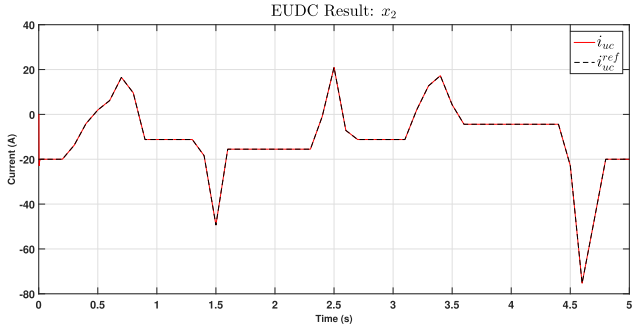

FIGURE 18. Plot of state i_{uc} (EUDC).

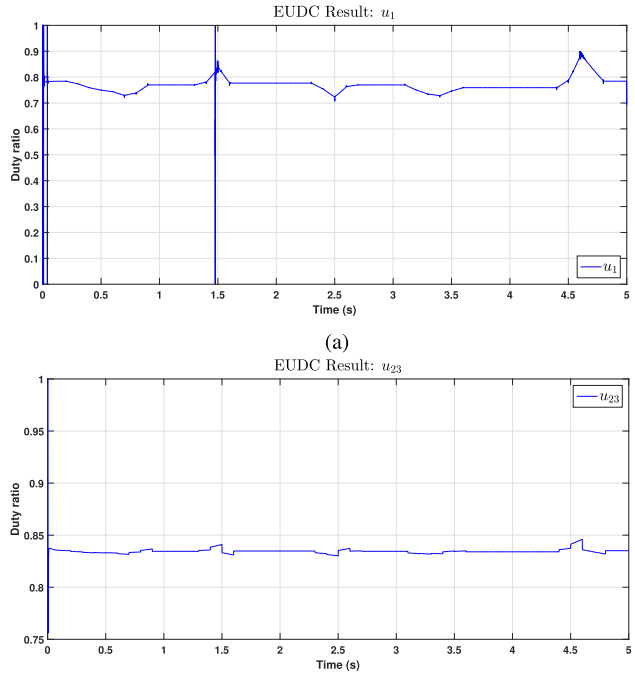

FIGURE 19. Plots of control signals (EUDC mode). (a) Plot of duty ratio u_1. (b) Plot of duty ratio u_{23}.

Here the FC provides the EUDC with the low frequency currents and the UC provides it with the high frequency currents. The low frequency part of the EUDC corresponds with lower current changes in the FC current waveform (Fig. 17) and the high load changes are provided by the UC (Fig. 18). The figure shows that the tracking performance of UC current

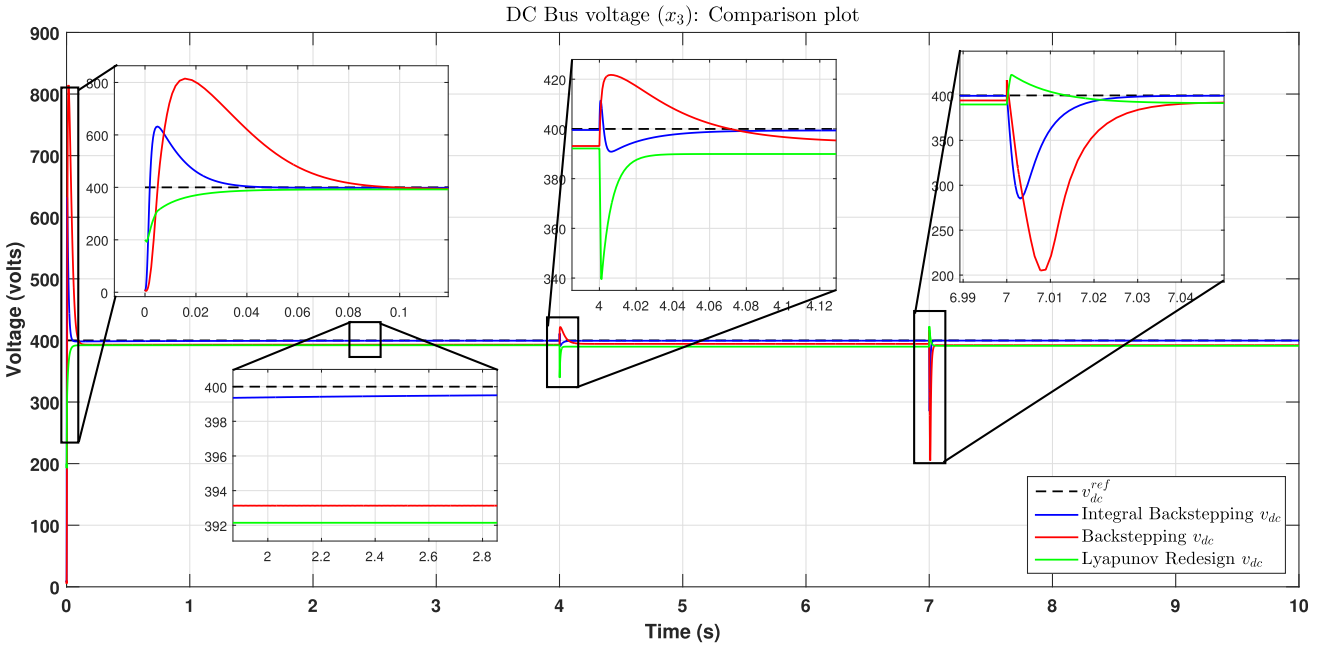

FIGURE 20. Comparison of the two proposed schemes with a previous study [22].

TABLE 5. Calculated accuracy of the three control schemes.

Control Scheme	Accuracy (in %)
Lyapunov based control	84.89 %
Backstepping control	88.6 %
Integral Backstepping control	97.48 %

which tracks the reference value very nicely. The zero corresponds to the charging/discharging modes of the UC. Upper half-plane represents the mode when it is discharging (where $I_o > i_{fc}$), whereas the lower half-plane corresponds to the mode responsible for charging of UC ($I_o < i_{fc}$). The fuel cell current (Fig. 17) always remains positive and caters the need of the vehicle whenever required. Hence our objective has been achieved using integral Backstepping controller. Figure 19 shows the plots of control inputs u_1 & u_{23} applied at the gate of MOSFET switches.

3) COMPARISON BETWEEN DIFFERENT CONTROL SCHEMES

In this part of the simulation, we compare the results of Lyapunov based nonlinear controller [22], Backstepping controller and integral backstepping controller. Since our primary objective is to regulate the output DC bus voltage (state x_3), we will compare the v_{dc} waveforms obtained using these three controllers.

Fig. 20 shows the DC bus voltage v_{dc} waveform obtained using three control techniques. It can be observed that the performance of the Integral Backstepping mode controller (blue colored signal) is the best among these controllers. A small steady state error can be seen in v_{dc} of the Integral Backstepping control scheme (fig. 20), whereas the other two controllers exhibit a relatively large steady state error. To quantify the performance of these controllers, trapezoidal rule of numerical integration has been applied to evaluate the accuracy of these controllers by the following relation:

$$\text{Accuracy} = \int_0^{t_f} e_{dc}\, dt = \int_0^{t_f} (v_{dc} - v_{dc}^{ref})\, dt = \sum_{k=1}^{N} \left[\frac{e_{dc}(k-1) + e_{dc}(k)}{2} (t(k) - t(k-1)) \right]$$

Table 5 gives the accuracy of each of the aforementioned control scheme. It is quite evident that the Integral Backstepping control gives the most accurate results as seen in 5. This accuracy measurement gives a good idea about the performance of each control scheme from the electrical side of the HEV. However, to calculate the total efficiency of the HEV system, one must consider the inverter and the traction/induction motor attached with the DC-bus. The derivation of a complete mathematical model including the traction motor mathematical model is not the scope of this study as it requires an extensive knowledge of electro-mechanical systems. This work is recommended in the future prospects of this study.

VI. CONCLUSION

In this research work, a nonlinear integral Backstepping controller has been proposed for energy management in the Proton Exchange Membrane Fuel Cell (main source) plus Ultra-Capacitor (auxiliary source) hybrid electric vehicle. DC-DC Buck-Boost power converter has been fixed between the power sources and the load, used to meet the transient load demands of the vehicle. Global asymptotic stability of the proposed controller has been presented using Lyapunov based stability theory. To show the performance of the pro-

posed control scheme, simulation results have been detailed using MATLAB/Simulink. These results show that integral Backstepping controller successfully removes steady state error which has been observed in case of conventional Backstepping controller. The proposed controller outperforms both the Backstepping and the Lyapunov Redesign based controllers ([22]). The proposed algorithm has also been tested/verified on European standard driving cycle which shows promising results.

For future, any new suitable topology or some other control technique (for instance sliding mode controller, super-twisting algorithm, state feedback linearization based algorithm, etc) may be used to get better efficiency and less computational complexity. Other combinations of energy sources with devices like flywheel, can also be used.

REFERENCES

[1] A. Emadi, S. S. Williamson, and A. Khaligh, "Power electronics intensive solutions for advanced electric, hybrid electric, and fuel cell vehicular power systems," *IEEE Trans. Power Electron.*, vol. 21, no. 3, pp. 567–577, May 2006.
[2] K. Rajashekara, "Hybrid fuel-cell strategies for clean power generation," *IEEE Trans. Ind. Appl.*, vol. 41, no. 3, pp. 682–689, May 2005.
[3] M. B. Camara, H. Gualous, F. Gustin, and A. Berthon, "Design and new control of DC/DC converters to share energy between supercapacitors and batteries in hybrid vehicles," *IEEE Trans. Veh. Technol.*, vol. 57, no. 5, pp. 2721–2735, Sep. 2008.
[4] M. Yoong *et al.*, "Studies of regenerative braking in electric vehicle," in *Proc. IEEE Conf. Sustain. Utilization Develop. Eng. Technol. (STUDENT)*, Nov. 2010, pp. 40–45.
[5] A. Emadi, L. J. Young, and K. Rajashekara, "Power electronics and motor drives in electric, hybrid electric, and plug-in hybrid electric vehicles," *IEEE Trans. Ind. Electron.*, vol. 55, no. 6, pp. 2237–2245, Jun. 2008.
[6] S. Lu, K. A. Corzine, and M. Ferdowsi, "A unique ultracapacitor direct integration scheme in multilevel motor drives for large vehicle propulsion," *IEEE Trans. Veh. Technol.*, vol. 56, no. 4, pp. 1506–1515, Jul. 2007.
[7] M. B. Camara, H. Gualous, F. Gustin, A. Berthon, and B. Dakyo, "DC/DC converter design for supercapacitor and battery power management in hybrid vehicle applications—Polynomial control strategy," *IEEE Trans. Ind. Electron.*, vol. 57, no. 2, pp. 587–597, 2010.
[8] S. K. Kollimalla, M. K. Mishra, and N. L. Narasamma, "Design and analysis of novel control strategy for battery and supercapacitor storage system," *IEEE Trans. Sustain. Energy*, vol. 5, no. 4, pp. 1137–1144, Oct. 2014.
[9] A. Payman, S. Pierfederici, F. Meibody-Tabar, and B. Davat, "An adapted control strategy to minimize DC-bus capacitors of a parallel fuel cell/ultracapacitor hybrid system," *IEEE Trans. Power Electron.*, vol. 26, no. 12, pp. 3843–3852, Dec. 2011.
[10] A. S. Samosir and A. H. M. Yatim, "Implementation of dynamic evolution control of bidirectional DC–DC converter for interfacing ultracapacitor energy storage to fuel-cell system," *IEEE Trans. Ind. Electron.*, vol. 57, no. 10, pp. 3468–3473, Oct. 2010.
[11] A. Tani, M. B. Camara, and B. Dakyo, "Energy management based on frequency approach for hybrid electric vehicle applications: Fuel-cell/lithium-battery and ultracapacitors," *IEEE Trans. Veh. Technol.*, vol. 61, no. 8, pp. 3375–3386, Oct. 2012.
[12] M. Zandi, A. Payman, J.-P. Martin, S. Pierfederici, B. Davat, and F. Meibody-Tabar, "Energy management of a fuel cell/supercapacitor/battery power source for electric vehicular applications," *IEEE Trans. Veh. Technol.*, vol. 60, no. 2, pp. 433–443, Feb. 2011.
[13] A. Khaligh, J. Cao, and Y. J. Lee, "A multiple-input DC–DC converter topology," *IEEE Trans. Power Electron.*, vol. 24, no. 3, pp. 862–868, Mar. 2009.
[14] F. Nejabatkhah, S. Danyali, S. H. Hosseini, M. Sabahi, and S. M. Niapour, "Modeling and control of a new three-input DC–DC boost converter for hybrid PV/FC/battery power system," *IEEE Trans. Power Electron.*, vol. 27, no. 5, pp. 2309–2324, May 2012.
[15] H. Armghan, I. Ahmad, A. Armghan, S. Khan, and M. Arsalan, "Backstepping based non-linear control for maximum power point tracking in photovoltaic system," *Sol. Energy*, vol. 159, pp. 134–141, Jan. 2018.
[16] H. Armghan, I. Ahmad, N. Ali, M. F. Munir, S. Khan, and A. Armghan, "Nonlinear controller analysis of fuel cell–battery–ultracapacitor-based hybrid energy storage systems in electric vehicles," *Arabian J. Sci. Eng.*, vol. 43, no. 6, pp. 3123–3133, 2018.
[17] F. Akar, Y. Tavlasoglu, E. Ugur, B. Vural, and I. Aksoy, "A bidirectional nonisolated multi-input DC–DC converter for hybrid energy storage systems in electric vehicles," *IEEE Trans. Veh. Technol.*, vol. 65, no. 10, pp. 7944–7955, Oct. 2015.
[18] L. Solero, A. Lidozzi, and J. A. Pomilio, "Design of multiple-input power converter for hybrid vehicles," *IEEE Trans. Power Electron.*, vol. 20, no. 5, pp. 1007–1016, Sep. 2005.
[19] R. Ferreira, A. Ferreira, and P. Barbosa, "'Comparative study of linear and non-linear control techniques applied to DC-DC boost converter as a voltage regulator," Tech. Rep.
[20] M. S. Khan, I. Ahmad, H. Armaghan, and N. Ali, "Backstepping sliding mode control of FC-UC based hybrid electric vehicle," *IEEE Access*, vol. 6, pp. 77202–77211, 2018.
[21] J. Cao and A. Emadi, "A new battery/ultracapacitor hybrid energy storage system for electric, hybrid, and plug-in hybrid electric vehicles," *IEEE Trans. Power Electron.*, vol. 27, no. 1, pp. 122–132, Jan. 2012.
[22] H. El Fadil, F. Giri, J. M. Guerrero, and A. Tahri, "Modeling and nonlinear control of a fuel cell/supercapacitor hybrid energy storage system for electric vehicles," *IEEE Trans. Veh. Technol.*, vol. 63, no. 7, pp. 3011–3018, Sep. 2014.
[23] M. Mohammedi, O. Kraa, M. Becherif, A. Aboubou, M. Ayad, and M. Bahri, "Fuzzy logic and passivity-based controller applied to electric vehicle using fuel cell and supercapacitors hybrid source," *Energy Procedia*, vol. 50, pp. 619–626, Jan. 2014.
[24] L.-K. Yi, J. Zhao, and D. Ma, "Adaptive backstepping sliding mode nonlinear control for buck DC/DC switched power converter," in *Proc. IEEE Int. Conf. Control Autom.*, May 2007, pp. 1198–1201.
[25] R. Skjetne and T. I. Fossen, "On integral control in backstepping: Analysis of different techniques," in *Proc. Amer. Control Conf.*, vol. 2, Jun. 2004, pp. 1899–1904.
[26] J. Liu, Y. Gao, X. Su, M. Wack, and L. Wu, "Disturbance-observer-based control for air management of PEM fuel cell systems via sliding mode technique," *IEEE Trans. Control Syst. Technol.*, vol. 27, no. 3, pp. 1129–1138, May 2019.
[27] S. Miret. (Nov. 2013). *Storage Wars: Batteries vs. Supercapacitors*. [Online]. Available: http://berc.berkeley.edu/storage-wars-batteries-vs-supercapacitors/
[28] D. Maksimović and R. W. Erickson, *Fundamentals of Power Electronics*. Springer, 2007.